ELSEVIER

PII: S0032-3861(97)00567-3

Polymer Vol. 39 No. 12, pp. 2615–2620, 1998

0032-3861/98/$19.00+0.00

Effect of chain end group hydrophobicity on surface aggregation structure of poly(styrene–*block*–4-vinylpyridine) symmetric diblock copolymer films

Xiqun Jiang, Keiji Tanaka, Atsushi Takahara and Tisato Kajiyama†*
Department of Materials Physics and Chemistry, Graduate School of Engineering, Kyushu University, 6-10-1 Hakozaki, Higashi-ku, Fukuoka 812-81, Japan
(Received 16 April 1997; revised 20 June 1997)

Proton-terminated polystyrene–*block*–poly(4-vinylpyridine) (P(St–*b*–4VP)-H) and 3,3,3-trifluoropropyldimethylsilane-terminated polystyrene–*block*–poly(4-vinylpyridine) (P(St–*b*–4VP)-C_2C^F) symmetric diblock copolymers were synthesized by a living anionic polymerization. Differential scanning calorimetry (DSC) measurements revealed that both diblock copolymers were in a microphase-separated state in the bulk. The results of X-ray photoelectron spectroscopy (XPS) measurements revealed that in the case of the P(St–*b*–4VP)-H film, the surface weight fraction of poly(4-vinylpyridine) (P4VP) decreased drastically on annealing at 432 K for 90 h in order to minimize the magnitude of the free energy at the air–polymer interface, whereas in the case of the P(St–*b*–4VP)-C_2C^F film, the surface P4VP weight fraction was almost the same as the bulk value even after annealing at 423 K for 90 h. Also, scanning force microscopy observations (SFM) were in good agreement with the XPS results. These results clearly indicate that the surface molecular aggregation state of the hydrophobic–hydrophilic diblock copolymer film can be controlled by the hydrophobicity of the chain end groups.

(Keywords: surface aggregation structure; chain end group; poly(styrene–*block*–4-vinylpyridine))

INTRODUCTION

Recently, the surface aggregation structure of block copolymer films has received increasing attention, and has been extensively investigated by using various techniques such as neutron reflectivity (NR)[1–3], X-ray photoelectron spectroscopy (XPS)[4–6], dynamic secondary ion mass spectrometry (DSIMS)[7], transmission electron microscopy (TEM)[8–10] and atomic force microscopy (AFM)[11–13]. Most studies have revealed that the molecular aggregation state at the air–polymer interface of block copolymer films is quite different from the bulk state, such as in the surface segregation of one component or surface-induced phase separation. Generally, in the case of a diblock copolymer film, the component with the lower surface free energy is enriched at the air–polymer interface in order to minimize the magnitude of the interfacial energy.

More recently, it has been revealed by DSIMS measurements[14] that the chain end groups were enriched in a depth range up to around twice the radius of gyration, R_g, from the outermost surface. Also, several groups reported the remarkable surface enrichment of fluoroalkyl chain end groups for blend films composed of PS and PS with perfluoroalkyl end groups, and it has been revealed that chain ends with low surface free energy localized at the film surface and the magnitude of the surface tension of the blend film was reduced due to the surface localization of low-surface-free-energy chain ends[15–17]. These results indicate that the chain end groups play an important role in the surface enrichment of one component of a polymer blend. However, all the systems mentioned above are blend systems; for a microphase-separated block copolymer having chain end groups with a low surface free energy, little work has been done up to the present on the chain end group effect on the surface aggregation state.

Here, in order to investigate the effect of the chain end group chemistry on surface structure, a symmetrical poly(styrene–*block*–4-vinylpyridine) diblock copolymer terminated with a proton (P(St–*b*–4VP)-H) and a chain end group with low surface free energy, $-CF_3$, (P(St–*b*–4VP)-C_2C^F) were synthesized by sequential anionic polymerization. Generally, the PS component in the P(St–*b*–4VP) film formed the outermost layer in order to minimize the surface free energy. By introducing a hydrophobic fluoromethyl group at the end of the hydrophilic P4VP block, the possibility of whether the end group orientation effect at the interface can compete with the formation of the PS layer at the surface can be confirmed and evaluated. The surface structure of the P(St–*b*–4VP)-H and P(St–*b*–4VP)-C_2C^F films was investigated on the basis of XPS measurements, and AFM and lateral force microscopy (LFM) observations.

EXPERIMENTAL

Materials

Styrene (St) and 4-vinylpyridine (4VP) were dried over CaH_2 for 24 h and then distilled twice under vacuum. The purified monomers were stored in an argon atmosphere. Just

* To whom correspondence should be addressed
† Tel.: + 81-92-642-3558; fax: + 81-92-651-5606; e-mail: tkajitcf@mbox.nc.kyushu-u.ac.jp

prior to use, the monomers were treated with triethylaluminium and again vacuum distilled. 1,1-Diphenylethylene (DPE) was vacuum distilled over CaH_2 and *n*-butyllithium. Tetrahydrofuran (THF) was distilled after refluxing for 24 h over sodium and benzophenone under a nitrogen atmosphere. *sec*-Butyllithium (*sec*-BuLi) and 3,3,3-trifluoropropyldimethylchlorosilane were used as received.

Polymerization

Poly(styrene–*b*–4-vinylpyridine) diblock copolymers terminated with neutral hydrogen or trifluoropropyldimethylsilane end group with low surface free energy were prepared by sequential anionic polymerization in THF under an argon atmosphere at 195 K using *sec*-BuLi as initiator.

Firstly, THF was transferred to a glass reactor by a capillary technique, then the reactor was cooled to 195 K and a calculated amount of *sec*-BuLi was added to the well-stirred THF solution by means of a syringe. Next, the desired amount of styrene monomer was added dropwise. After 60 min at 195 K, DPE was added to the reactor. Then, 10 min later, 4-vinylpyridine as the second monomer was added to the reactor. After 3 h at 195 K, a 3–5 fold excess of methanol or 3,3,3-trifluoropropyldimethylchlorosilane was added to the reactor in order to prepare the proton-terminated P(St–*b*–4VP) or 3,3,3-trifluoropropylsilane-terminated P(St–*b*–4VP) diblock copolymers. These were then precipitated in hexane and vacuum dried.

Characterization of diblock copolymer

The number-average molecular weight, M_n and the molecular weight distribution, M_w/M_n of the synthesized diblock copolymers, where M_w denotes the weight-average molecular weight, were determined by gel permeation chromatography (g.p.c.; L-6000;, Hitachi Co., Ltd.) measurements with dimethyl formamide (DMF) as eluent, employing calibration with polystyrene standards. Also, the bulk P4VP weight fraction was determined by nuclear magnetic resonance (n.m.r.; GSX-400; JEOL Co., Ltd.) measurements from DMF-d_7 solution.

The thin diblock copolymer films were prepared by a spin-coating method from DMF solution on to a silicon wafer with a native oxide layer at room temperature. The film thickness before annealing was measured by using an ellipsometer (M-150; Jasco Co., Ltd.). The diblock copolymer films were dried for 48 h at room temperature and then vacuum dried at 343 K for 24 h. An equilibration state with respect to surface molecular aggregation was obtained by annealing the thin films at 423 K for 90 h under vacuum.

In order to evaluate the bulk T_g of the diblock copolymers, differential scanning calorimetry (d.s.c.; Rigaku thermoflex 8230) measurements were performed. The specimen was heated to 453 K at a heating rate of 5 K min^{-1} under a nitrogen purge.

The surface chemical composition of the diblock copolymer films was evaluated by carrying out XPS

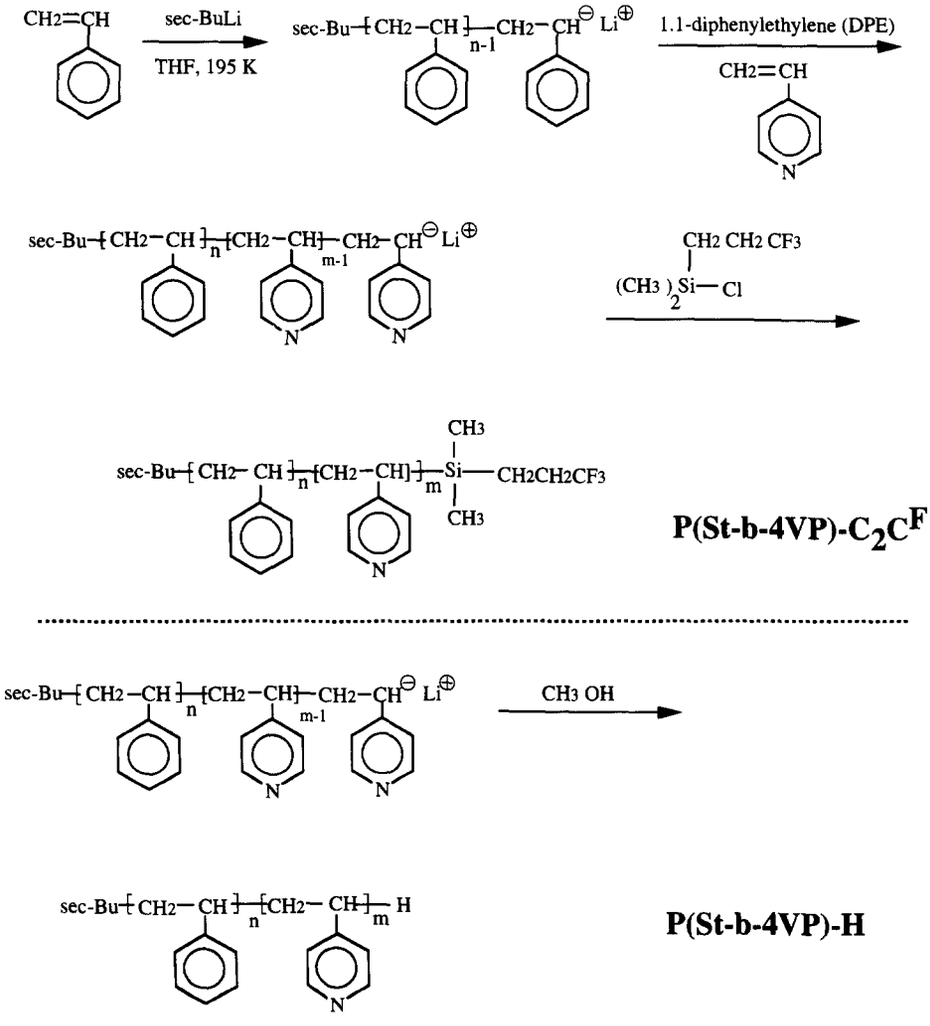

Scheme 1 Synthesis of the end-functionalized diblock polymer

(ESCA-850; Shimadzu Co., Ltd.) measurements with Mg Kα radiation at 8 kV and 30 mA. The spectrometer chamber was maintained at 10^{-6} Pa. The analytical depths ($d = 3\lambda \sin\theta$) were calculated by using the value of the inelastic mean free path (λ) evaluated from Ashley's equation[18]. The magnitudes of d were 4.8 nm, 6.8 nm and 9.7 nm corresponding to photoelectron emission angles of 30°, 45° and 90°, respectively. The values of the surface weight fractions of P4VP, ω, in the diblock copolymer films were calculated by using the following equation

$$\frac{I_N}{I_C} = \frac{\omega/M_{P4VP}}{[8(1-\omega)/M_{PS}] + (7\omega/M_{P4VP})}$$

where I_N and I_C are the integrated intensities of the nitrogen and carbon atoms, respectively, in the core-electron photoemission spectrum, and M_{PS} and M_{P4VP} are the molecular weights of the styrene and vinylpyridine repeating units, respectively.

The surface morphology of the thin diblock copolymer films was investigated by using AFM and LFM. The AFM and LFM images were obtained by use of an SPA 300 with an SPA 3700 controller. The AFM and LFM cantilever used was microfabricated from Si_3N_4, and its spring constant was 0.025 N m^{-1}. The AFM and LFM observations were carried out in a repulsive force range of around 1 nN.

The surface free energies of PS and P4VP are 40.2 mJ m^{-2} and 68.2 mJ m^{-2}, respectively, determined by static contact angle measurements by Owens' procedure[19].

RESULTS AND DISCUSSION

Synthesis of end-functionalized diblock copolymer

Scheme 1 describes the synthesis route of the P(St–*b*–4VP)-H and P(St–*b*–4VP)-C_2C^F diblock copolymers. The living polystyryl anions (PSt^-) were prepared by the polymerization of styrene monomer, with *sec*-BuLi as initiator, in THF at 195 K for 60 min. In order to avoid any side reactions during the anionic polymerization of 4VP, DPE was added to the PSt^- solution. The colour of the solution changed immediately from orange to deep red, which indicated the conversion of PSt^- to PS–DPE^-, and 4VP monomer was then added to the polymerization medium. After the reaction was allowed to proceed for 3 h, 3,3,3-trifluoromethyldimethylchlorosilane as terminator was added to the living polymerization solution in order to functionalize the chain end group of the P(St–*b*–4VP) diblock copolymer. Unexpectedly, the deep yellow colour, which was characteristic of $P4VP^-$, did not disappear instantaneously and remained even after 30 min at 195 K. Finally, the deep yellow colour of the solution disappeared after reaction for 1 h at room temperature due to the low rate of the reaction between the $P4VP^-$ and the terminator. Since THF is not a good solvent for P4VP, it is expected that diblock copolymer anions formed the micelles, being composed of PS as the arms and $P4VP^-$ as the cores in THF. Thus, since only the 3,3,3-trifluoromethyldimethylchlorosilane molecules diffusing through the micelle arms can react with P4VP anions, the termination reaction by 3,3,3-trifluoromethyldimethylchlorosilane may proceed slowly.

The polymer obtained was carefully precipitated from THF solution into hexane and was then purified by Soxhlet extraction with cyclohexane in order to remove any PS homopolymer and unreacted terminating agents, because cyclohexane is a solvent only for PS. *Table 1* shows the characterization of the diblock copolymers P(St–*b*–4VP)-H and P(St–*b*–4VP)-C_2C^F employed in the present study. The magnitudes of M_n for P(St–*b*–4VP)-H and P(St–*b*–4VP)-C_2C^F were 41k and 14k, respectively, and the magnitudes of M_w/M_n were 1.11 and 1.13, respectively. These results indicate that the synthesized diblock copolymers have a narrow molecular weight distribution and the side reaction was suppressed by PS–DPE precursors during the polymerization of the 4VP monomer. The bulk P4VP weight fraction of the diblock copolymers was determined to be 49.5% for P(St–*b*–4VP)-H and 51.0% for P(St–*b*–4VP)-C_2C^F, based on ^{1}H n.m.r. measurements. In addition, the functionality of the fluorosilane end group evaluated from the ^{1}H n.m.r. spectrum was 0.8 for P(St–*b*–4VP)-C_2C^F. Thus, both the P(St–*b*–4VP)-H and the P(St–*b*–4VP)-C_2C^F diblock copolymers have a well-defined chemical structure.

Bulk characterization

Figure 1 shows d.s.c. curves for the P(St–*b*–4VP)-H and P(St–*b*–4VP)-C_2C^F films. The temperature at the midpoint of the baseline shift was defined as the bulk glass transition temperature, T_g. In both cases, two T_gs were observed. The lower T_gs of 379.2 K and 380.9 K for P(St–*b*–4VP)-H and P(St–*b*–4VP)-C_2C^F, respectively, were assigned to the PS component, while the higher T_gs of 395.4 K and 394.5 K for P(St–*b*–4VP)-H and P(St–*b*–4VP)-C_2C^F, respectively, were assigned to the P4VP component. These results indicate that the bulk P(St–*b*–4VP)-H and P(St–*b*–4VP)-C_2C^F films were in a microphase-separated state even though the molecular weights were not high, and they also suggest that a relatively large magnitude of χ and a relatively large repulsion between the two different segments occurred for the P(St–*b*–4VP) system.

Table 1 Results of the characterization of the end-functionalized diblock copolymers

Sample	M_n^a	M_w/M_n^b	PVP content[c] (wt.%)
P(St–*b*–4VP)-H	41k	1.11	49.5
P(St–*b*–4VP)-C_2C^F	14k	1.13	51.0

[a]Diblock copolymer molecular weights are determined by g.p.c. analysis of PS block and ^{1}H n.m.r. analysis of diblock copolymers[b]Determined by g.p.c.[c]Based on ^{1}H n.m.r. analysis

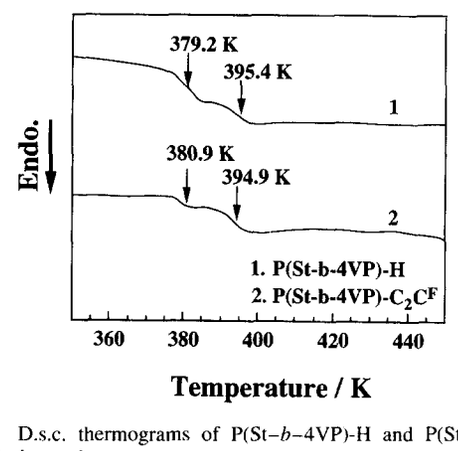

Figure 1 D.s.c. thermograms of P(St–*b*–4VP)-H and P(St–*b*–4VP)-C_2C^F diblock copolymers

Surface chemical composition and surface structure of end-functionalized diblock copolymer thin film

The surface chemical compositions of the proton-terminated P(St–*b*–4VP)-H and 3,3,3-trifluoropropyldimethylsilane-terminated P(St–*b*–4VP)-C_2C^F films were investigated by carrying out XPS measurements. *Figure 2* shows typical XPS C_{1s} and N_{1s} spectra for the P(St–*b*–4VP)-H, P(St–*b*–4VP)-C_2C^F and P4VP homopolymer thin films. The C 1s and N_{1s} peaks were observed at about 285.0 ev and 399.0 ev, respectively. The slight peak observed at 291.5–292.0 ev in the C 1s spectra was assigned to the π–π^* transition of the benzene ring. It is apparent from the spectra that the order of the relative peak intensity ratio of N 1s to C 1s is P4VP homopolymer > P(St–*b*–4VP)-C_2C^F > P(St–*b*–4VP)-H. These differences allow the analysis of the surface compositions of the P(St–*b*–4VP)-H and the P(St–*b*–4VP)-C_2C^F films. The surface P4VP fraction was calculated using the equation mentioned above based on the XPS measurements.

Figure 3 shows the surface P4VP fraction in the as-cast P(St–*b*–4VP)-H and P(St–*b*–4VP)-C_2C^F thin films. The emission angle of the photoelectrons was 90°. In order to investigate the surface structure being in a quasi-equilibrium state, an annealing treatment of the films was carried out at 423 K for 90 h. The surface P4VP fraction in the annealed P(St–*b*–4VP)-H and the P(St–*b*–4VP)-C_2C^F films was also plotted in *Figure 3*. In the case of the as-cast P(St–*b*–4VP)-H film, since the surface P4VP fraction was lower than the bulk fraction of 49.5%, it appears that the PS component is somewhat segregated at the film surface in order to minimize the surface free energy. On the other hand, the surface P4VP fraction in the as-cast P(St–*b*–4VP)-C_2C^F film was in the range from 47 to 56%, with the magnitude being almost comparable to the bulk magnitude, and no apparent film thickness dependence of the surface composition was observed. Thus, it appears that the surface aggregation state of a diblock copolymer film can be controlled by the chemistry of the chain end group.

After annealing, the surface P4VP fraction in the P(St–*b*–4VP)-H film decreased remarkably in comparison with that in the as-cast one, indicating that the annealing treatment induces preferential surface segregation of the PS component with lower surface free energy. On the other hand, in the case of the annealed P(St–*b*–4VP)-C_2C^F film, the surface P4VP fraction decreased slightly after the annealing treatment. This might be explained by the preferential surface segregation of 3,3,3-trifluoropropyldimethylsilane-terminated P4VP due to an extremely low surface free energy of the CF_3 end group. On the basis of a theoretical calculation[20] and recent experimental results[21], it has been revealed that chain end groups tend to localize at the surface if the surface free energy of the chain end group is lower than that of the main chain. Since the surface free energy of the CF_3 end group is the lowest among block polymer components such as the PS, P4VP and the CF_3 end groups, the CF_3 end group is localized at the air–polymer interface. Thus, it seems reasonable to conclude that the PS component was not preferentially or inherently enriched at the film surface of the P(St–*b*–4VP)-C_2C^F film even after annealing at 423 K for 90 h because the CF_3 end group was connected to the P4VP blocks by a covalent bond.

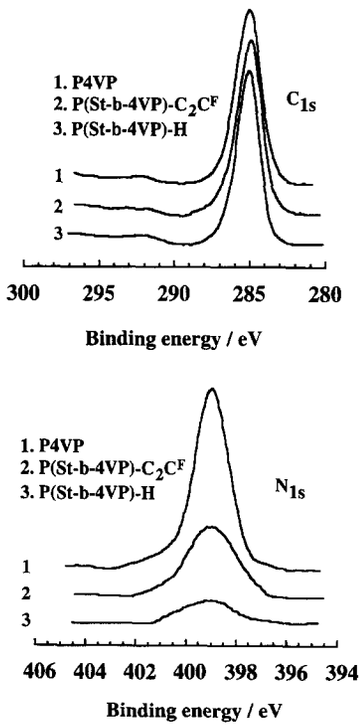

Figure 2 XPS C_{1s} and N_{1s} core-level spectra of the P4VP homopolymer, and the P(St–*b*–4VP)-H and P(St–*b*–4VP)-C_2C^F copolymers after annealing at 423 K for 90 h

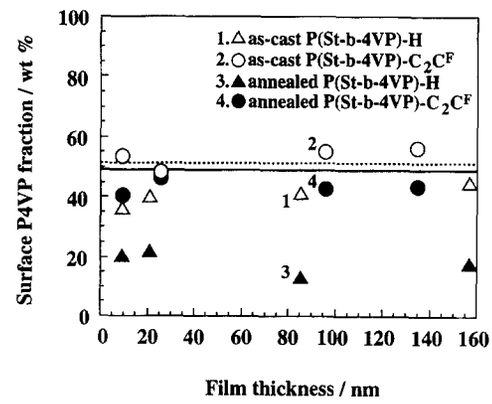

Figure 3 Surface P4VP fraction in the P(St–*b*–4VP)-H and P(St–*b*–4VP)-C_2C^F thin films of various thicknesses, before and after annealing. The solid and the dotted lines denote the bulk composition of the P(St–*b*–4VP)-H and P(St–*b*–4VP)-C_2C^F films, respectively

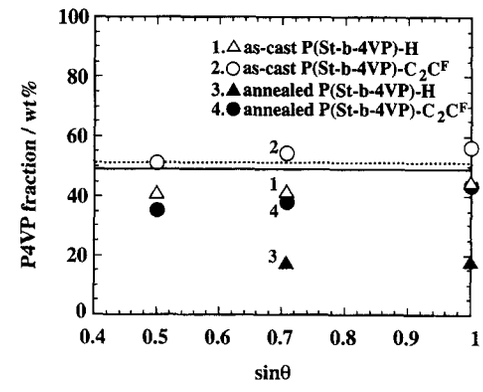

Figure 4 Angular dependence, sin θ, of the P4VP fraction in the P(St–*b*–4VP)-H thin film of thickness 157 nm and the P(St–*b*–4VP)-C_2C^F film of thickness 135 nm, before and after annealing. The solid and the dotted lines denote the bulk composition of the P(St–*b*–4VP)-H and P(St–*b*–4VP)-C_2C^F films, respectively

Figure 4 shows the angular dependence, $\sin\theta$, of the surface P4VP fractions for the P(St–*b*–4VP)-H thin film of thickness 157 nm, and that for the P(St–*b*–4VP)-C_2C^F thin film of thickness 135 nm, before and after annealing. The values of $\sin\theta$ of 0.50, 0.71 and 1.0 correspond to the analytical depth ranges 0–4.8 nm, 0–6.8 nm and 0–9.7 nm, respectively. The analytical depth dependence of the surface composition was not clearly detected in all cases. Also, the surface composition of the as-cast films almost corresponded to the bulk one. This result indicates that a randomly oriented microphase-separated structure was formed at the as-cast film surface. After annealing, the surface P4VP fraction in the P(St–*b*–4VP)-H film was remarkably low in comparison with that in the as-cast one. Moreover, in the case of a $\sin\theta$ of 0.5, corresponding to a closer analytical depth range of 0–4.8 nm from the air–polymer interface, the N_{1s} peak for P4VP was not clearly observed. Therefore, it seems reasonable to consider that in the case of the annealed P(St–*b*–4VP)-H, the surface enrichment of PS gradually increased on approaching the film surface from the bulk. On the other hand, in the case of the annealed P(St–*b*–4VP)-C_2C^F thin film, the surface P4VP fractions were 35.3%, 38.0% and 43.5% at $\sin\theta$ of 0.5, 0.7 and 1.0, respectively, *i.e.* the surface P4VP fraction slightly decreased with a decrease in analytical depth. Thus, it can be considered that the PS component may be somewhat enriched at the film surface. However, it should be noted that a fair amount of P4VP was still present at the film surface due to the surface localization of low-surface-free-energy chain end groups being covalently bonded to the P4VP blocks.

Figure 5 shows (*a*) AFM and (*b*) LFM images of the P(St–*b*–4VP)-H film of thickness 157 nm after an annealing treatment at 423 K for 90 h. In the AFM image, a protruding region 200–300 nm wide and 4–6 nm high was observed at the film surface. However, in the LFM image, the surface was homogenous on the several tens of nanometres scale; in other words, almost no clear contrast was observed. Since the outermost surface is covered with the PS component, as was shown from the XPS results mentioned above, it seems reasonable to conclude that a contrast was not observed in the LFM image, even though both a bright and a dark region were present in the AFM image.

Figure 6 shows (*a*) AFM and (*b*) LFM images of the P(St–*b*–4VP)-C_2C^F thin film after the annealing treatment at 423 K for 90 h. Many small protrusions 90–150 nm wide and 5–7 nm in height were observed in the AFM image. The larger protrusions 300–500 nm in width and 7–9 nm high seem to be formed by coalescence of the small protrusions. In the LFM image, a clear contrast was observed due to the presence of both PS and P4VP components at the air–polymer interface. The brighter and darker parts in the LFM image correspond to higher and lower lateral force regions, respectively. Since the area fraction of the bright region is about 30% in the LFM image, which is consistent with a surface P4VP fraction based on XPS measurements of P(St–*b*–4VP)-C_2C^F, and, furthermore, the brighter region in the AFM image corresponds to the darker region in the LFM image, it is reasonable to conclude that the P4VP component corresponds to a higher lateral force component, and the brighter and darker regions in the LFM image are composed of P4VP and PS components. respectively. That is, the protruding regions in *Figure 6(a)* are composed of the PS domains of P(St–*b*–4VP)-C_2C^F. These results apparently indicate that the surface aggregation structure and the surface mechanical properties of P(St–*b*–4VP)-H and P(St–*b*–4VP)-C_2C^F are strongly influenced by the chemical structure of the chain end group.

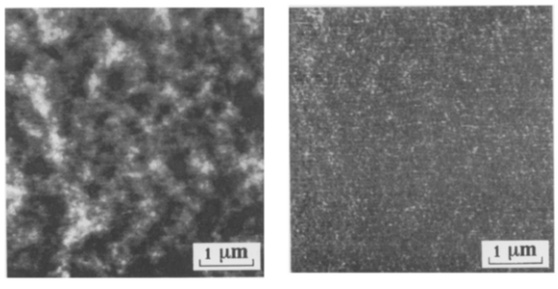

(a) AFM image **(b) LFM image**

Figure 5 (a) AFM and (b) LFM images of the P(St–*b*–4VP)-H thin film of thickness 157 nm, after annealing at 423 K for 90 h

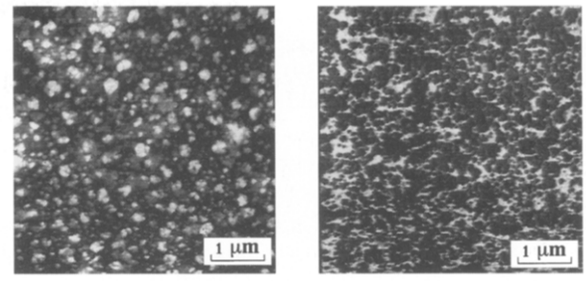

(a) AFM image **(b) LFM image**

Figure 6 (a) AFM and (b) LFM images of the P(St–*b*–4VP)-C_2C^F thin film of thickness 135 nm, after annealing at 423 K for 90 h

CONCLUSIONS

Symmetric P(St–*b*–4VP)-H and P(St–*b*–4VP)-C_2C^F diblock copolymers were synthesized by sequential anionic polymerization. Angular dependent XPS measurements and SFM observations revealed that in the case of P(St–*b*–4VP)-H thin films, the film surface was almost completely covered with the PS component after an annealing treatment at 423 K for 90 h. On the other hand, in the case of the P(St–*b*–4VP)-C_2C^F thin films, the films exhibited a heterogeneous surface structure, the P4VP component was also present at the film surface in an amount close to the bulk composition, and surface enrichment of the PS component could not be attained. Also, LFM observations indicate that the region composed of the P4VP component shows a higher lateral force.

These result indicate that the surface aggregation structure of block copolymers strongly depends on the end group chemistry. The surface localization of chain end groups with a low surface free energy increased the surface fraction of the P4VP block with a higher surface free energy. Therefore, by designing the end group structure of block copolymers, the surface aggregation structure can be controlled.

ACKNOWLEDGEMENTS

We would like to express our sincere thanks to Professors Akira Hirao and Sei-ichi Nakahama for their kind advice on anionic polymerization. Also, this work was partially

supported by a Grant-in-Aid for Scientific Research on Priority Areas 'New Polymers and Their Nano-organized System' (no. 277/08246239), from the Ministry of Education, Science, Sports and Culture, Japan.

REFERENCES

1. Koneripalli, N., Singh, N., Levicky, R., Bates, F. S., Gallagher, P. D. and Satija, S. K., *Macromolecules*, 1995, **28**, 2897.
2. Mayes, A. M., Johnson, R. D., Russell, T. P., Smith, S. D., Satija, S. K. and Majkrzak, C. F., *Macromolecules*, 1993, **26**, 1047.
3. Torikai, N., Noda, I., Karim, A., Satija, S. K., Han, C. C., Matsushita, Y., Kawakatsu, T., *Macromolecules*, 1997, **30**, 2909.
4. Green, P. F., Christensen, T. M., Russell, T. P. and Jerome, R., *Macromolecules*, 1989, **22**, 2189.
5. Tanaka, K., Takahara, A. and Kajiyama, T., *Acta Polym.* , 1995, **46**, 476.
6. Thomas, H. R. and O'Malley, J. J., *Macromolecules*, 1979, **12**, 323.
7. Coulon, G., Russell, T. P., Deline, V. R. and Green, P. F., *Macromolecules*, 1989, **22**, 2581.
8. Hasegawa, H. and Hashimoto, T., *Macromolecules*, 1985, **18**, 589.
9. Henkee, C. S. and Thomas, E. L., *J. Mater. Sci.*, 1988, **23**, 1685.
10. Mori, H., Hirao, A., Nakahama, S. and Senshu, K., *Macromolecules*, 1994, **27**, 4093.
11. Collin, B., Chatenay, D., Coulon, G., Ausserre, D. and Gallot, Y., *Macromolecules*, 1992, **25**, 1621.
12. Leclere, Ph., Lazzaroni, R. and Bredas, J. L., *Langmuir*, 1996, **12**, 4317.
13. Nick, L., Lippitz, A., Unger, W., Kindermann, A. and Fuhrmann, J., *Langmuir*, 1995, **11**, 1912.
14. Tanaka, K., Taura, A., Ge, S. -R., Takahara, A. and Kajiyama, T., *Macromolecules*, 1996, **29**, 3040.
15. Sugiyama, K., Hirao, A. and Nakahama, S., *Makromol. Chem. Phys.*, 1996, **197**, 3149.
16. Elman, J. F., John, B. D., Long, T. E. and Koberstein, J. T., *Macromolecules*, 1994, **27**, 5341.
17. Schaub, T. F., Kellogg, G. J., Mayes, A. M., Kulasekere, R., Ankner, J. F. and Kaiser, H., *Macromolecules*, 1996, **29**, 3982.
18. Ashley, J. C., *IEEE Trans. Nucl. Sci.*, 1980, **NS-27**, 1454.
19. Owens, D. K. and Wendt, R. C., *J. Appl. Polym. Sci.*, 1969, **13**, 1741.
20. Kumar, S. K., Vacatello, M. and Yoon, D. Y., *Macromolecules*, 1990, **23**, 2189.
21. Hunt, M. O., Belu, A. M. Jr., Linton, R. W. and DeSimone, J. M., *Macromolecules*, 1993, **26**, 4854.